

Discrete Particle Methods for Simulating High-Velocity Impact Phenomena

*M.O. Steinhauser^{1,2}

¹Fraunhofer Institute for High-Speed Dynamics, Ernst-Mach-Institute, EMI, Freiburg, Germany

²Department of Chemistry, University of Basel, Switzerland

*Presenting author: martin.steinhauser@emi.fraunhofer.de

Abstract

In this paper we introduce a mesh-free computational model for the simulation of high-speed impact phenomena. Within the framework of particle dynamics simulations we model a macroscopic solid ceramic tile as a network of overlapping discrete particles of microscopic size. Using potentials of the Lennard-Jones type we integrate the classical Newtonian equations of motion and perform uni-axial, quasi-static load simulations to customize our three model parameters to the typical tensile strength, Young's modulus and the compressive strength of a ceramic. Subsequently we perform shock load simulations in a standard experimental set-up, the edge-on impact (EOI) configuration. Our obtained results concerning crack initiation and propagation through the material agree well with corresponding high-speed EOI experiments with Aluminum Oxinitride (AlON), Aluminum Oxide (Al_2O_3) and Silicon Carbide (SiC), performed at the Fraunhofer Ernst-Mach-Institute (EMI). Additionally, we present initial simulation results where we use our particle-based model to simulate a second type of high-speed impact experiments where an accelerated sphere strikes a thin aluminum plate. Such experiments are done at our institute to investigate the debris clouds arising from such impacts, which constitute a miniature model version of a generic satellite structure that is hit by debris in the earth's orbit. Our findings are that a discrete particle based method leads to very stable, energy-conserving simulations of high-speed impact scenarios. Our chosen interaction model seems to work particularly well in the velocity range where the local stresses caused by impact shock waves markedly exceed the ultimate material strength.

Keywords: Computer Simulation, Discrete particle model, Multiscale modeling, High-speed impact, Molecular Dynamics, Hypervelocity.

Introduction

Understanding the mechanisms of failure in materials on various length- and time scales is a prerequisite for the design of new materials with desired superior properties such as high toughness or strength. On the macroscopic scale, many materials such as concrete or ceramics may be viewed as being homogeneous; however, on the scale of a few microns these materials often exhibit an inhomogeneous polyhedral granular structure which is known to influence its macroscopic mechanical and/or optical properties [1]. Whether a material under load displays a ductile, metal-like behavior or ultimately breaks irreversibly, in essence depends on the atomic crystal structure and on the propagation of defects in the material. Broken atomic bonds (cracks) and dislocations are the two major defects determining mechanical properties on an atomic scale. Due to the ever increasing computing power of modern hardware, many-particle molecular dynamics (MD) simulations taking into account the degrees of freedom of several billion atoms are nowadays feasible [2][3]. Molecular dynamics investigations of this type using generic models of the solid state have lead to a basic understanding of the processes that govern failure and crack behavior, such as the dynamical instability of crack tips [4][5], the limiting speed of crack propagation[6]-[8], the dynamics of dislocations [9][10], or the universal features of energy dissipation in fracture [11]. However, investigations of materials which

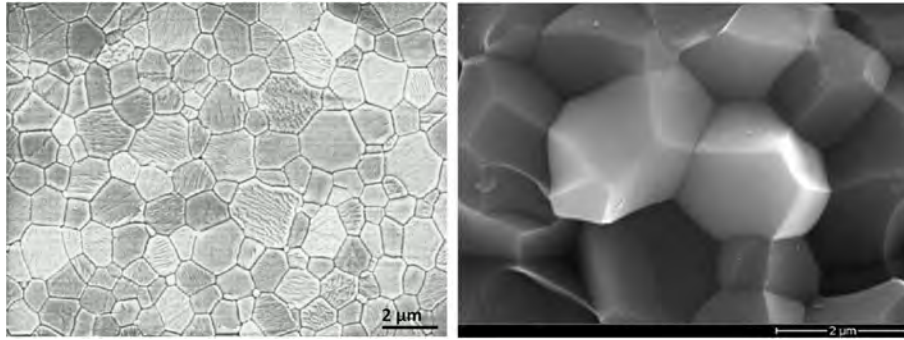


Figure 1: Left: Photomicrograph of an Al_2O_3 ceramic tile. Right: 3D view of the polyhedral granular surface structure of Al_2O_3 .

involve multiple structure levels, such as polycrystalline solids, require very large ensembles of atoms to accurately reflect the structures on the microscopic and mesoscopic levels [12]. For systems of reasonable size, atomistic simulations are still limited to following the dynamics of the considered systems only on time scales of nanoseconds. Such scales are much shorter than what is needed to follow many dynamic phenomena that are of experimental interest [13][14]. On the microscale, the typical structure of many brittle materials is composed of convex polyhedra, as seen in two-dimensional (2D) photomicrographs of polycrystalline ceramics (Fig. 1).

High-Performance Ceramics (HPC)s

With ceramics, the specific shape and size of their polycrystalline grain structures is formed in a sintering process where atomic diffusion plays a dominant role. Usually the sintering process results in a porous microstructure with grain sizes of several hundred micrometers. Using a nano-sized fine-grained granulate as a green body along with an adequate process control, it is possible to minimize both, the porosity (which is smaller than 0.05% in volume), as well as the generated average grain size (smaller than 1 μm). It is known that both leads to a dramatic increase in hardness which outperforms most metal alloys at considerably lower weight and thus yields a HPC such as AlON, Al_2O_3 , SiC or Boron Carbide (B4C). Characteristic for HPCs are an extremely low porosity (less than 0.1% in volume), high purity, and high hardness of the final macroscopic structure. An additional beneficial property of HPCs is the fact that, depending on the final grain size, the ceramics exhibit translucency or even complete transparency which renders these materials the prime source for future engineering applications [15][16]. Typical applications of HPCs that benefit from high hardness at low weight are e.g. wear resistant brake discs, protection shields in the automobile industry or bone substitutes in medical devices.

The use of extremely small grain sizes below 100 nm in the making of HPCs results again in decreasing hardness [16]. Hence, there is no simple connection between grain size and hardness of a polycrystalline material. As a consequence, today, one is compelled to search for the optimal micro structure for a specific application by intricate and expensive experimental trial-and-error studies. Some of the mechanical properties of HPCs are measured at EMI by means of ballistic high-speed impact experiments in the experimental standard set-up of the EOI configuration, where a fast impactor hits the edge of a ceramic tile of typical dimension $(10 \times 10 \times 2) \text{ cm}^3$, cf. Fig. 2.

Here, the ceramic specimens are placed at a distance of 1cm in front of the muzzle of a gas gun in order to achieve reproducible impact conditions. In this set-up the rear of the projectile is still guided by the barrel gun when the front hits the target.

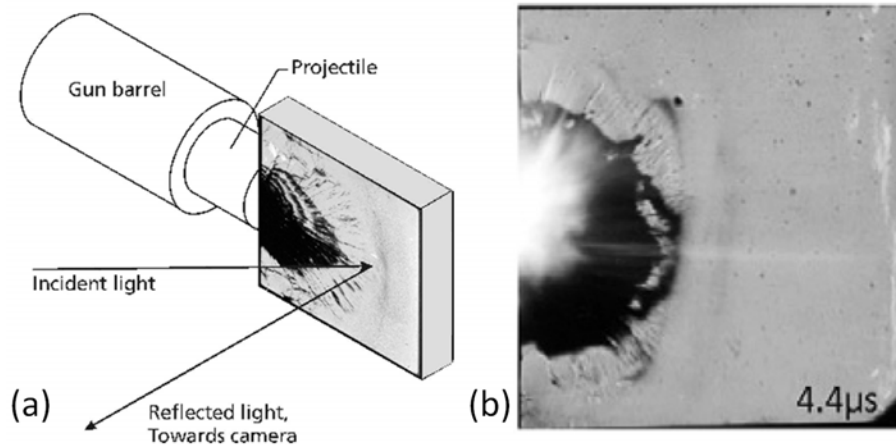


Figure 2: (a) The edge-on impact (EOI) configuration for the reflected light set-up. (b) Sample high-speed photograph of an EOI experiment with SiC impacted at striking velocity 1040 m/s displaying the propagating shock wave through the material.

Modeling and Simulation of Granular Microstructures

With numerical investigations taking explicitly into account the microstructural details, one can expect to achieve a considerably enhanced understanding of the structure-property relationships of such materials [17][18]. For simulations of macroscopic material behavior, techniques based on a continuum approximation, such as the Finite Element Method (FEM) or Smooth Particle Hydrodynamics (SPH), are almost exclusively used. In a continuum approach the considered grain structure of the material is typically subdivided into smaller (finite) elements, e.g. triangles in 2D or tetrahedra in 3D. Upon failure, the elements are separated according to some predefined failure modes, often including a heuristic Weibull distribution [19], which is artificially imposed upon the system. Results using these methods are usually strongly influenced by mesh resolution and mesh quality [20]. On the other hand, classical molecular dynamics (MD) simulations based on Newtonian dynamics of particles have been shown to capture the occurring physical phenomena of shock waves in solids correctly, but are usually limited to the nanoscale and to timescales which are too small to allow for a direct comparison with experiments.

Particle Simulations of Failure in Polycrystalline Materials

In our approach to modeling impact failure of polycrystalline, brittle materials such as ceramics, we use the framework of classical particle dynamics simulations.

Particle Model

Using Occams Razor, instead of trying to directly reproduce the geometrical shape of grains of ceramics as seen in photomicrographs, cf. Fig. 1, we model the solid state as an unordered network of monodisperse soft particles with radii r , connected by non-linear elements (springs) which are allowed to overlap in the initial random configuration, see Fig. 3.

The initial random degree of overlap between each particle pair and determines the force needed to detach these particles from each other. The force is imposed on the particles by elastic springs. This simple model can easily be extended to incorporate irreversible changes of state such as plastic flow. However, for brittle materials, where catastrophic failure occurs after a short elastic strain, plastic flow behavior can be neglected. The initial disc overlap and thus the overall density of the model solid can be adjusted by a compactness parameter as dimensionless input parameter of the simulation model. In the example in Fig. 3, $\rho = 0.5$. The same overall system configuration can then be visualized as a network of links that connects the centers of overlap-

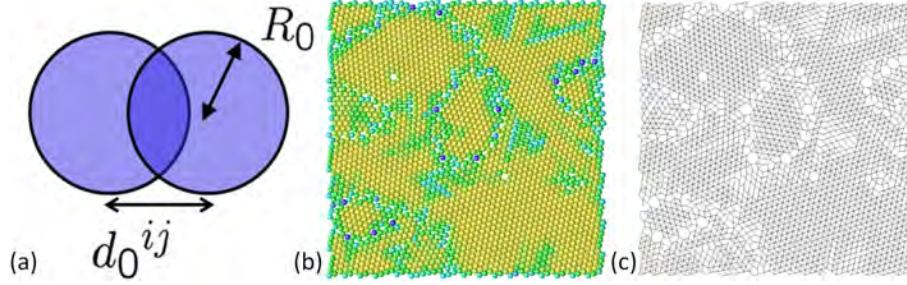


Figure 3: (a) Scheme of overlapping soft particles. (b) Realization of an initial particle configuration in the simulation with $N = 2500$ and $\Theta = 0.9$. The color code displays the structure in terms of nearest next neighbors (coordination number): blue: 0, green: 2, and yellow: 4. (c) The corresponding illustration of the system as unordered network of links.

ping particles. This way of modeling a solid composed of particles was originally used for the simulation of granular flow problems in geophysical models by Cundall and Strack [21], often referred to as the Discrete Element Method (DEM). Though DEM is very closely related to the MD method, it is generally distinguished by its inclusion of rotational degrees-of-freedom, of complicated contact forces and often complicated geometries (including polyhedra).

Potentials and Scaling Properties

As a fundamental requirement for our particle model we demand to have very few parameters which model the basic material properties of a brittle ceramic material; in essence, these are first, the resistance to pressure, second, the cohesive forces that keep the material constituents together, and then the microscopic failure. A material resistance against pressure is introduced by a Lennard-Jones-type repulsive potential

$$V_R^{ij}(d^{ij}) = \alpha R_0^3 \left[\left(\frac{d_0^{ij}}{d^{ij}} \right)^{12} - 2 \left(\frac{d_0^{ij}}{d^{ij}} \right)^6 + 1 \right] \quad (1)$$

which acts on every pair $\{ij\}$ of particles for $0 < d^{ij} \leq d_0^{ij}$ and which vanishes for $d^{ij} > d_0^{ij}$, i. e. for particle pairs which do not overlap. Factor α (which relates to the compressive strength) in Eqn. (1) scales the energy density and the pre-factor R_0^3 ensures the correct scaling behavior of the calculated total stress $\sigma_{ij}\sigma^{ij} = \sum_{ij} F^{ij}/A$ in the system (with A being the area where the force F^{ij} is applied), independent of the number of particles N . The cohesive potential is modeled by a harmonic function $V_C^{ij}(d^{ij})$, given that there are no irreversible changes of state when the material is submitted to small external forces. Each pair of particles $\{ij\}$ can be visualized as being connected by a spring, the equilibrium length of which equals the initial distance d_0^{ij} , cf. Fig. 3. Thus, for $d^{ij} > 0$ we have:

$$V_C^{ij}(d^{ij}) = \beta R_0 \left(d^{ij} - d_0^{ij} \right)^2. \quad (2)$$

In Eqn. (2) parameter β (which has the dimension [energy/length] and relates to the tensile strength of the material) determines the strength of the potential and the pre-factor R_0 again ensures proper scaling behavior of the macroscopic physical material response, e.g. the stress-strain curve upon external load, for details, see Steinhauser [12]. We demonstrate this model property in Fig. 4 which displays the stress-strain relation obtained for different realizations of solids with a different number of particles. The idea of this particular scaling of the potential

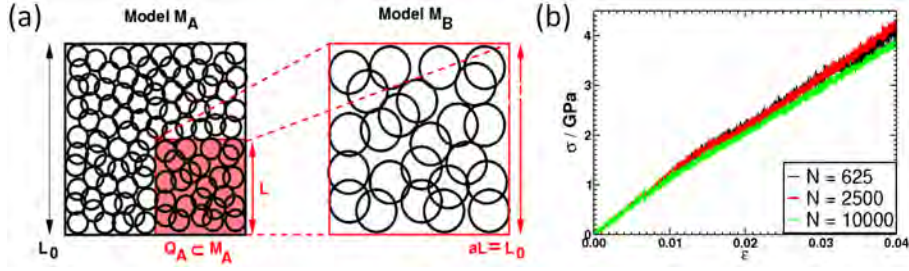


Figure 4: (a) Illustration of the scaling property of our particle model. A number of particles of a small subset $Q_A \subset M_A$ of the original model M_A are enlarged, until they are of the same size as the original system. The resulting system M_B contains fewer particles than M_A , but the macroscopic physical properties, e.g. Young's modulus stay the same upon external load. (b) Averaged stress-strain curves obtained from simulations of systems with different number of particles. $N = 625, 2500, 10^4$, $\alpha = 20$, $\beta = 350$. The slope of the different realizations is in essence independent of N .

is that one should always obtain the same macroscopic physical properties of a system, e.g. the same stress-strain relation, independent of the arbitrarily chosen number of particles which represent the solid. As a result of this, when up- or downscaling our system, i.e. when changing the number of particles, it is not necessary to re-adjust the pre-factors α and β in the potentials of Eqn. (1) and (2).

Finally we consider failure in our model by introducing two breaking thresholds for the springs with respect to compressive and to tensile failure. If either of these thresholds is exceeded, the respective spring is defined as broken and is removed from the system. A simple tensile criterion is reached when the overlap between two particles vanishes, i.e. when the distance between two particle centers exceeds the sum of their constant radii:

$$d^{ij} > 2R_0. \quad (3)$$

Failure under pressure load occurs when the actual mutual particle distance is less by a factor γ than the initial mutual distance, i.e. when

$$d^{ij} < \gamma /, d_0^{ij}, \quad (4)$$

where ($0 < \gamma < 1$). Parameter γ is later fitted to reproduce Young's modulus of the real material. We note that the repulsive potential is independent from the failure criteria of Eqn. (3) and (4), i.e. even if bonds described by Eqn. (2) are broken in the system due to pressure or tensile failure, the involved particles still interact via the repulsive potential of Eqn. (1) and cannot artificially move through each other.

Initial Configurations

For our numerical analysis, we simulate directly the experimental geometry of the edge-on impact configuration (EOI) as shown in Fig. 2. We use as initial configuration a random distribution of particles in a cubic simulation box. Generally, we observe an increase in the number of pronounced peaks in the distribution of initial particle distances d_0^{ij} when parameter Θ is increased, as shown in Fig. 5. This clearly indicates a change of the initial structure, i.e. of the arrangement and packing density of particles in the system. In Fig. 5 we display the coordination numbers for two initial realization of a brittle, granular solid at two different densities. Thus, by fine-tuning parameter Θ , one can fix the density ρ of the model material according to

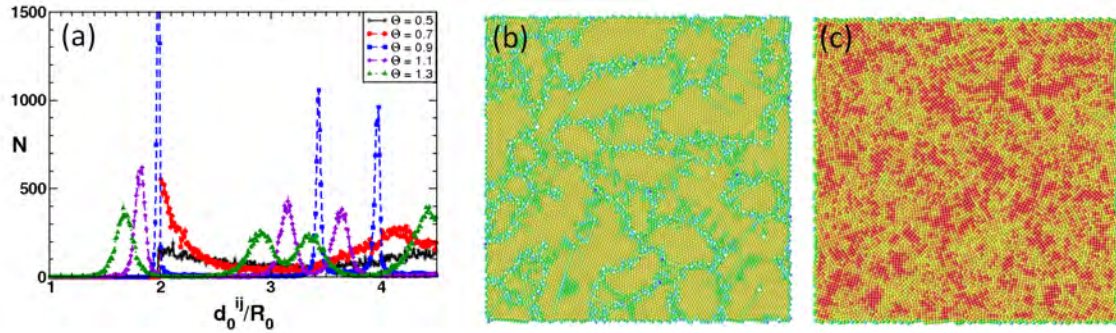


Figure 5: (a) Distribution of mutual initial distances for different values of θ in a system with particles. (b) Sample initial configurations with and with a preferred hexagonal arrangement of soft particles. The color code displays the coordination number within the range 4-6 (yellow to green). (c) Another realization with the same θ , coordination numbers 6-8 (green to red) and with a predominantly quadratic packing.

the one obtained in sintered ceramics of interest, e.g. in the case of Al_2O_3 , the experimental density ρ is typically is larger than 98% in volume.

High-Speed Impact Simulations

By adjusting the three free model parameters α , β , γ to experimental values typical for HPC materials, one is able to obtain the correct stress–strain relationship of a specific material as observed in (macroscopic) biaxial loading experiments. After this fixing of parameters the model is applied to other types of external loading, e.g. ballistic high–speed impact in the EOI configuration or a direct impact which can be used as a model system for investigating the situation of a satellite being hit by space debris. This is done with no further model adjustments, and the results are compared with experimental findings. In Fig. 6 we present non–equilibrium molecular dynamics simulation (NEMD) results for a SiC system with impact velocity $v = 150\text{m/s}$ using $N = 10^5$ particles in a direct comparison with corresponding high–speed experimental results. In general, one can conclude that the physics of shock wave propagation is captured rather well in the simulations, opening a route to a detailed quantitative investigation of observed shock wave and failure phenomena in brittle materials, for example by investigating the number of broken bonds in the system as displayed in the bottom row of part (a) in Fig. 6. Part (b) of Fig. 6 analyzes the ratio of broken bonds to the total number of initial bonds for SiC and Al_2O_3 for different impact velocities and system sizes. The percentage of failed bonds which can be considered as a simple measure for the degree of failure in the material, is consistently larger for SiC, which agrees well with experimental findings.

Finally, in Fig. 7 we show a 3D series of simulation snapshots of the developing debris cloud resulting from a direct ballistic impact of a spherical particle onto a plate, directly after the impact occurred. Debris from the impactor is colored in red and gray particles represent the target. The long–term purpose of this type of impact simulations is to develop a computational model that reproduces the debris cloud distribution which is observed in corresponding high–speed ballistic experiments. This is important for evaluating satellite safety in the earth’s orbit, where a continuously increasing number of debris particles increase the risk of collisions with satellites.

Figure 8 displays a typical experimental high–speed photograph of a ballistic impact experiment, shortly after the impact occurred. One can clearly see the debris cloud forming. For comparison we have displayed the debris cloud obtained from a simulation snapshot.

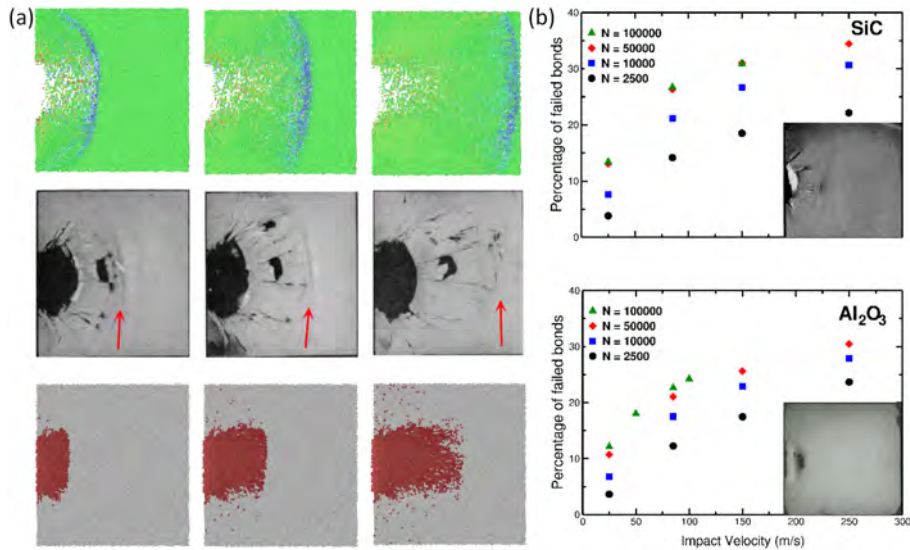


Figure 6: (a) Top row: Simulation results of a SiC EOI simulation at $v = 150\text{m/s}$. The material is hit at the left edge. A shock wave (color-coded in blue) propagates through the system. The time interval between the individual snapshots from left to right is $2\mu\text{s}$. Middle row: The same experiment with a real SiC specimen. The time interval between the photomicrographs is comparable with the ones in the top row. Arrows indicate the location of the shock wave front. Bottom row: The same computer simulation, this time displaying the occurring damage in the material with respect to broken bonds. (b) Degree of damage at $3\mu\text{s}$ after impact for SiC and Al_2O_3 for different N and impact velocities. The insets show high-speed camera snapshots indicating the corresponding degree of damage in the materials at striking velocity $v = 85\text{m/s}$.

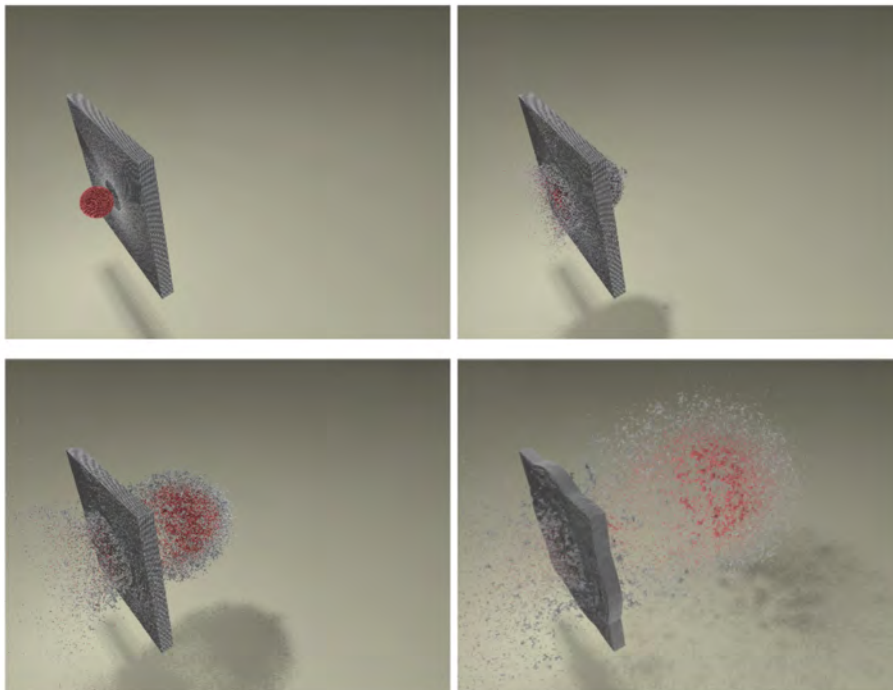


Figure 7: A series of 3D simulation snapshots showing a sphere impacting a plate at very high speed ($v = 6.7\text{km/s}$) in a ballistic impact simulation. Red indicates impactor particles and gray indicates target plate particles.

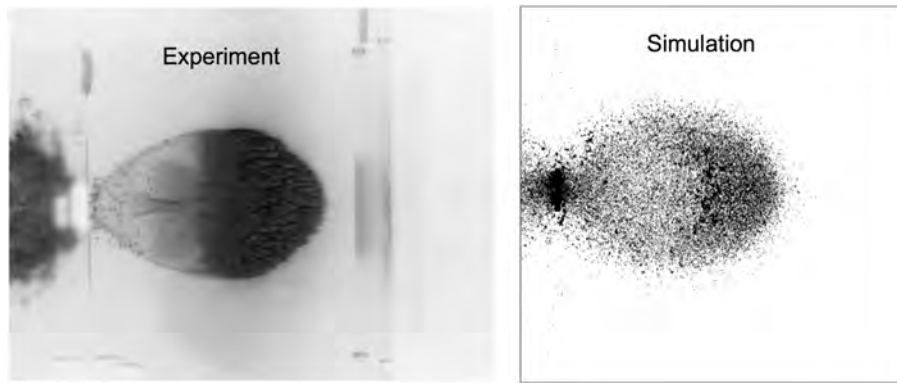


Figure 8: Left: Experimental snapshot of the debris cloud. Right: Realization of this ballistic impact experiment in our particle-based computer simulation.

Conclusions

The proposed simulation scheme in this paper, which uses discrete particles to model the basic properties of a solid, has proven to be stable and convergent. It allows for studying in detail the fracture and failure mechanisms of brittle materials. The simulated failure dynamics, shock wave propagation and the degree of damage with the proposed three-parameter model are in good agreement with experimental findings, albeit in the presented study for the edge-on-impact configuration, only moderate velocities are used to impact the material, as here, we want to demonstrate the principal usefulness of the proposed model by fitting its parameters to a specific, brittle ceramic material. In a first attempt to go to very high impact velocities (larger than 6km/s, which is sometimes called *hypervelocity impact*) we have presented a ballistic impact simulation which results in the formation of a debris cloud. Here, we also find good numerical stability of the proposed particle model and reasonable agreement with corresponding ballistic impact experiments.

In future investigations, it is planned to extend the proposed modeling approach to the simulation of yet larger impact velocities and to other, more complex materials, such as compounds, e.g. fiber-reinforced SMCs (Sheet Moulding Compounds) or to structures typically encountered in soft matter, e.g. biological bilayer membranes, which exhibit much more complex microstructural features.

Acknowledgements

We acknowledge financial support by the German Aerospace Center (DLR) under grant number 50LZ1502 "DEM-O".

References

- [1] Steinhauser, M. O and Grass, K. (2005) Failure and plasticity models of ceramics: A numerical study. In: Khan A, Kohei S, Amir R., editors, Dislocations, Plasticity, Damage and Metal Forming, Materials Response and Multiscale Modeling. Neat Press, Fulton, ML USA, pp. 370–373.
- [2] Abraham, F. F, Walkup R., Gao, H., Duchaineau, M., De La Rubia, T. D., Seager, M. (2002) Simulating materials failure by using up to one billion atoms and the worlds fastest computer: Brittle fracture. *Proc. Natl. Acad. Sci.* **99**, 5777–5782.
- [3] Kadau, K., Germann, T. C., Lomdahl, P.S. (2006) Molecular dynamics comes of age: 320 billion atom simulation on BlueGene/L. *Int J. Mod. Phys. C* **18**, 1755–1761.
- [4] Fineberg, J. Materials science: Close-up on cracks. (2003) *Nature* **426**, 131–132.
- [5] Buehler, M. J., Gao, H. Dynamical fracture instabilities due to local hyperelasticity at crack tips. (2006) *Nature* **439**, 307–310.

- [6] Abraham, F. F., Brodbeck, D., Rafey, R. A., Rudge, W. E. Instability dynamics of fracture: A computer simulation investigation. (1994) *Phys. Rev. Lett.* **73**, 272–275.
- [7] Abraham, F. F., Gao, H. How fast can cracks propagate? (2000) *Phys. Rev. Lett.* **84**, 3113–3116.
- [8] Rosakis, A. J., Samudrala, O., Coker, D. (1999) Cracks faster than the shear wave speed. *Science* **284**, 1337–1340.
- [9] Abraham, F. F., Schneider, D., Land, B., Lifka, B., Skovira, J., Gerner, J., Rosenkrantz, M. (1997) Instability dynamics in three-dimensional fracture: An atomistic simulation. *J. Mech. Phys. Solids* **45**, 1461–1471.
- [10] Bulatov, V., Abraham, F. F., Kubin, L., Devrince, B., Yip, S. (1998) Connecting atomistic and mesoscale simulations of crystal plasticity. *Nature* **391**, 669–672.
- [11] Gross, S. P., Fineberg, J., Marder, M., McCormick, W. D., Swinney, H. L. (1991) Acoustic emissions from rapidly moving cracks. *Phys. Rev. Lett.* **71**, 3162–3165.
- [12] Steinhauser M. O. (2008) *Computational Multiscale Modeling of Fluids and Solids Theory and Applications*, Springer, Heidelberg, Berlin, New York.
- [13] Zhou, S. J., Beazley, D. M., Lomdahl, P. S., Holian, B. L. (1997) Large-scale molecular dynamics simulations of three-dimensional ductile failure. *Phys. Rev. Lett.* **78**, 479–482.
- [14] Zhou, S. J., Preston, D. L., Lomdahl, P. S., Beazley, D. M. (1998) Large-Scale molecular dynamics simulations of dislocation intersection in copper. *Science* **279**, 1525–1527.
- [15] Krell, A., Blank, P., Ma, H., Hutzler, T., van Bruggen, M., Apetz, R. (2003) Transparent sintered corundum with high hardness and strength. *J. Am. Chem. Soc.* **86**, 12–18.
- [16] Krell, A., Blanck, P., Ma, H. W., Hutzler, T., Nebelung, M. (2003) Processing of high-density submicrometer Al₂O₃ for new applications. *J. Am. Ceram. Soc.* **86**, 546–553.
- [17] Chen, M., McCauley, J. W., Hemker, K.J. (2003) Shock-induced localized amorphization in boron carbide. *Science* **299**, 1563–1566.
- [18] Bringa, E. M., Caro, A., Wang, Y., Victoria, M., McNaney, J. M., Remington, B. A., Smith, R. F., Torralva, B. R., Van Swygenhoven, H. (2005) Ultrahigh strength in nanocrystalline materials under shock loading. *Science* **309**, 1838–1841.
- [19] Weibull, W. A statistical distribution function of wide applicability. (1951) *J. Appl. Mech.* **18**, 293–297.
- [20] Steinhauser, M. O., Hiermaier, S. (2009) A review of computational methods in materials science: Examples from shock-wave and polymer physics. *Int. J. Mol. Sci.* **10**, 5135–5216.
- [21] Cundall, P. A., Strack, O. D. L. (1979) A discrete numerical model for granular assemblies. *Geotechnique* **29** 47–65.